Distinct cerebral perfusion patterns in FTLD and AD

W.T. Hu, MD, PhD*
Z. Wang, PhD*
V.M.-Y. Lee, PhD, MBA
J.Q. Trojanowski, MD, PhD
J.A. Detre, MD
M. Grossman, MD

Address correspondence and reprint requests to Dr. Murray Grossman, Department of Neurology–2 Gibson, Hospital of the University of Pennsylvania, 3400 Spruce St., Philadelphia, PA 19104-4283
mgrossma@mail.med.upenn.edu

ABSTRACT

Objective: We examined the utility of distinguishing between patients with frontotemporal lobar degeneration (FTLD) and Alzheimer disease (AD) using quantitative cerebral blood flow (CBF) imaging with arterial spin labeled (ASL) perfusion MRI.

Methods: Forty-two patients with FTLD and 18 patients with AD, defined by autopsy or CSF-derived biomarkers for AD, and 23 matched controls were imaged with a continuous ASL method to quantify CBF maps covering the entire brain.

Results: Patients with FTLD and AD showed distinct patterns of hypoperfusion and hyperperfusion. Compared with controls, patients with FTLD showed significant hypoperfusion in regions of the frontal lobe bilaterally, and hyperperfusion in posterior cingulate and medial parietal/precuneus regions. Compared with controls, patients with AD showed significant hypoperfusion in the medial parietal/precuneus and lateral parietal cortex, and hyperperfusion in regions of the frontal lobe. Direct comparison of patient groups showed significant inferior, medial, and dorsolateral frontal hypoperfusion in FTLD, and significant hypoperfusion in bilateral lateral temporal-parietal and medial parietal/precuneus regions in AD.

Conclusions: Doubly dissociated areas of hypoperfusion in FTLD and AD are consistent with areas of significant histopathologic burden in these groups. ASL is a potentially useful biomarker for distinguishing patients with these neurodegenerative diseases. *Neurology*® 2010;75:881–888

GLOSSARY

Aβ42 = β-amyloid$_{1-42}$; **AD** = Alzheimer disease; **ASL** = arterial spin labeling; **bvFTD** = behavioral-variant frontotemporal dementia; **cASL** = continuous arterial spin labeling; **CBS** = corticobasal syndrome; **CBF** = cerebral blood flow; **dACC** = dorsal anterior cingulate cortex; **dlPFC** = dorsolateral prefrontal cortex; **FDR** = false detection rate; **FTLD** = frontotemporal lobar degeneration; **GM** = gray matter; **iFC** = inferior frontal cortex; **MCI** = mild cognitive impairment; **MNI** = Montreal Neurological Institute; **mTC** = middle temporal cortex; **OFC** = orbital frontal cortex; **PC** = parietal cortex; **PCA** = principal component analysis; **PCC** = posterior cingulate cortex; **PPA** = primary progressive aphasia; **PRC** = precuneus; **PVE** = partial volume effect; **t-tau** = total tau; **TE** = echo time; **TI** = inversion time; **TR** = repetition time; **WM** = white matter.

Frontotemporal lobar degeneration (FTLD) is the most common cause of progressive cognitive decline in young-onset dementia. Because Alzheimer disease (AD) accounts for 30% of cases presenting with a clinical diagnosis of primary progressive aphasia (PPA) or behavioral-variant frontotemporal dementia (bvFTD),[1,2] it is important to distinguish between FTLD and AD so that appropriate treatments can be initiated. This distinction is difficult on clinical grounds alone, because AD can mimic PPA and bvFTD,[1,2] and FTLD can present with a memory disorder.[3]

Structural MRI has been used to help distinguish between autopsy-defined FTLD and AD,[4,5] but structural atrophy often emerges in more advanced disease stages. Variability in absolute brain volume increases in aging, so absolute measurements of cortical volume can be difficult to interpret.[5,6] In contrast, measures of regional brain function may provide greater

Supplemental data at www.neurology.org

*These authors contributed equally to this article.

From the Departments of Neurology (W.T.H., J.A.D., M.G.), Pathology (W.T.H., V.M.-Y., J.Q.T.), Psychiatry (Z.W.), and Radiology (J.A.D.), University of Pennsylvania School of Medicine, Philadelphia, PA. Dr. Hu is currently with the Department of Neurology, Emory University, Atlanta, GA.

Study funding: Supported by the NIH (AG17586, AG15116, NS44266, NS53488, R03DA023496, and 5P30NS045839) and an AAN Clinical Research Fellowship.

Disclosure: Author disclosures are provided at the end of the article.

sensitivity to degenerative disease. PET is frequently used for this purpose,[7] but this involves exposure to ionizing radiation and is not widely available.

Another biomarker of regional brain function is cerebral blood flow (CBF), which is usually tightly coupled to brain metabolism.[8] Arterial spin labeling (ASL) perfusion MRI allows noninvasive quantification of CBF. In this study, we used histopathology or validated CSF biomarkers for AD as the gold standard for defining group membership. We compared perfusion profiles in patients with FTLD and AD relative to controls and to each other. We used a continuous ASL technique[9] at 3 T to increase sensitivity compared with prior studies.[10]

METHODS

Standard protocol approvals, registrations, and patient consents. All protocols were approved by the University of Pennsylvania Institutional Review Board, and informed consent was obtained from all patients and designated representatives.

Subjects. Patients were recruited from the Department of Neurology at University of Pennsylvania School of Medicine. All patients were evaluated prospectively by neurologists with expertise in progressive neurodegenerative syndromes (M.G. and W.H.). Clinical diagnosis was based on published criteria.[11,12] Seventy-three patients were initially identified with a clinical spectrum disorder consistent with FTLD, including a disorder of social comportment and personality (bvFTD), PPA, or corticobasal syndrome (CBS), or with clinically probable AD. The diagnosis of each patient was confirmed through a consensus mechanism. Autopsy information became available in 6 patients (4 FTLD, 2 AD), using methods summarized previously,[13] whereas others underwent CSF evaluation for levels of AD biomarkers (total tau [t-tau] and β-amyloid$_{1\text{-}42}$ [Aβ42], n = 67). Using a reference set of patients with autopsy diagnosis and genetically mediated disease, patients in the current study were considered to have CSF biomarkers consistent with AD if the CSF t-tau–to–Aβ42 ratio was greater than 1.45, as empirically determined.[13] The remainder were considered to have a non-AD CSF profile, in keeping with FTLD in the current clinical context. After preliminary image analysis for brain coverage, 12 patients with FTLD and 1 patient with AD were excluded from analyses reported below, resulting in cohorts of 42 patients with FTLD (bvFTD = 25, PPA = 15, CBS = 2) and 18 patients with AD (bvFTD = 1, PPA = 11, CBS = 5). Because we aimed to determine the ASL pattern associated with underlying pathology, we analyzed patients according to pathology rather than clinical phenotypes. We also recruited 30 cognitively healthy seniors; 7 controls were excluded because of suboptimal brain coverage, resulting in a control cohort of 23. Demographic characteristics of patients and controls are summarized in table 1. Statistical analysis was performed using SPSS 12.0 (SPSS, Inc., Chicago, IL) unless otherwise specified. Chi-square tests and 1-way analysis of variance were used to evaluate demographic features.

Table 1 Mean (±SD) clinical characteristics of patients and controls

	Frontotemporal lobar degeneration (n = 42)	Alzheimer disease (n = 18)	Healthy seniors
Age, y	61.00 ± 8.47	61.94 ± 8.29	63.87 ± 8.00
Education, y	15.17 ± 2.79	16.72 ± 3.10	15.22 ± 2.35
Disease duration,[a] mo	46.40 ± 32.54	32.17 ± 16.83	NA
MMSE (max = 30)	23.46 ± 7.53	22.12 ± 6.73	28.85 ± 0.95
CSF biomarker levels			
Total tau, pg/mL	271.10 ± 375.21	546.75 ± 244.07	NA
p-tau$_{181}$, pg/mL	69.35 ± 39.68	164.43 ± 103.89	
Aβ42, pg/mL	350.76 ± 108.36	154.82 ± 50.25	
Total tau/Aβ42 ratio	0.69 ± 0.38	3.85 ± 2.14	

Abbreviations: Aβ42 = β-amyloid$_{1\text{-}42}$; MMSE = Mini-Mental State Examination; NA = not applicable.
[a] Disease duration was determined at the time of imaging by both subjective report and collateral history of symptom onset provided by a caregiver.

Imaging assessment and analysis. High-resolution structural MRI and quantitative ASL perfusion MRI were obtained from patients with AD or FTLD and from age-matched controls using a Siemens Trio 3-T whole-body magnetic resonance scanner (Siemens AG, Erlangen, Germany) with a product transmit/receive head coil. Structural imaging was performed with a T1-weighted 3-dimensional magnetization-prepared rapid acquisition gradient echo sequence with repetition time (TR)/inversion time (TI)/echo time (TE) = 1,620/950/3 milliseconds, flip angle = 30°, matrix = 192 × 256 × 160, and voxel size = 0.98 × 0.98 × 1 mm^3. Forty resting label/control image pairs were acquired using an amplitude-modulated continuous ASL (cASL) perfusion MRI sequence[14] with labeling time = 2 seconds, postlabeling delay = 1,500 milliseconds, field of view = 22 cm, matrix = 64 × 64 × 16, flip angle = 90°, TR = 3 seconds, TE = 17 milliseconds, slice thickness = 6 mm, and interslice space = 1.5 mm.

In-house software[15] based on MATLAB (The MathWorks, Natick, MA) and SPM5 (Wellcome Department of Cognitive Neurology, London, UK) were used for imaging analysis. Data from several patients were excluded from analysis because the prescribed slice coverage did not include the entire hippocampus and medial temporal cortex. CBF maps with poor quality after the following processing were also excluded if there was extensive head motion at most of the time points (>70%). Empirical cutoffs for excessive head motion were translation >4 mm, rotation >4°, between control and label translation >1 mm, and between control and label rotation >1°. MRI images of each session were realigned to the mean control image to correct for head movement and were spatially smoothed with a 3-dimensional isotropic gaussian kernel with full-width at half-maximum of 5 mm. Estimated head motion time courses were orthogonalized to periodically alternating labeling and control of the ASL paradigm. The cleaned motion time courses were then filtered out from the realigned ASL data using linear regression to remove residual head motion effects. Spatial-temporal noise reduction was then performed using principal component analysis (PCA).[16] The nonzero eigenvalue associated eigenvectors and their time courses were extracted by applying PCA along the spatial dimension of ASL data to avoid the computational problem of applying PCA along the temporal dimension.[17] Each image was projected into these eigenvectors to obtain the corresponding representation coefficients. The following criteria were used to discard the noise-related eigenvectors and the corresponding representing coefficients to further denoise the raw

ASL data: 1) any eigenvectors whose time courses were correlated with the zigzagged label-control paradigm were reserved, and 2) minor components of the remaining eigenvectors were discarded if they accounted for less than 1% of the total variance of the data before PCA denoising. Quantitative CBF image series were then calculated using a modified 2-compartment cASL perfusion model[9,14] with a simple-subtraction method. The time courses of the relative head motion between adjacent tag-control images were filtered out from the CBF image series to remove the residual motion effects. Temporal smoothing was then applied to improve the temporal signal-to-noise ratio at each voxel. The remaining CBF images were averaged to produce a mean CBF map for each subject. Structural images were normalized to a local template generated from the patients with AD, patients with FTLD, and age-matched controls. An exponentiated Lie algebra algorithm (DARTEL)[18] was applied to derive a local appearance template directly from the data set along with transformations from the template to each image.

To correct the partial volume effects (PVEs) introduced by the large voxel size used in ASL MRI, each individual subject's structural image was segmented into gray matter (GM), white matter (WM), and CSF based on the customized local template. The corresponding GM, WM, and CSF probability maps were then registered and subsampled to the native ASL MRI space. The resampled GM probability maps were thresholded at 0.3 to locate the GM voxels for the following PVE correction. Assuming a global ratio of 0.4 between WM perfusion and GM perfusion based on a previous PET study,[19] PVEs on GM CBF were corrected using the method proposed by Du et al.[10] with the following equation: $I_{corr} = I_{uncorr}/(PGM + 0.4 \cdot PWM)$, where I_{corr} and I_{uncorr} are the corrected and uncorrected intensities, and PGM and PWM are the tissue probabilities obtained by segmenting the structural images as described above. Because CBF signal in ASL MRI is derived from the ratio of ΔM to M0, PVE correction was also applied to the M0 images. We used a theoretical model based on the Bloch equations[20] to estimate tissue signal based on the acquisition parameters TR/TE and the relaxation rates (T1, T2) of each different tissue: $M_{tissue} = \rho \cdot \exp(-TE/T2) \cdot (1 - \exp(-TR/T1))$, where ρ is the water content in the tissue and was chosen to be 0.82, 0.72, and 1 for GM, WM, and CSF.[21] T1/T2 at 3 T for GM, WM, and CSF was chosen to be 1,110/60, 1,600/80, and 4,136/1,442 milliseconds.[22] We denoted the observed M0 intensity in WM by $MGM_{un} = PGM \cdot MGM + PWM \cdot MWM + PCSF \cdot MCSF$. Using the theoretical model, both MWM and MCSF can be represented as linear functions of MGM, and the above equation can be then re-expressed as $MGM_{un} = ratio \cdot MGM$, where $ratio = PGM + r_{W2G} \cdot PWM + r_{C2G} \cdot PCSF$, $r_{W2G} = MWM/MGM$, and $r_{C2G} = MCSF/MGM$ can be easily derived from the theoretical model. The PVE correction equation was then extended as $I_{corr} = I_{uncorr}/(PGM + 0.4 \cdot PWM) \cdot ratio$, and was used in this study.

The transformation derived from the structural image-based spatial normalization was used to normalize the CBF maps into the template space. The volume changes caused by the transformation were corrected using the modulation option in the DARTEL package to adjust CBF signal in areas that were compressed or expanded during image normalization.[18,23] The peak of each suprathreshold cluster was identified. The local template was mapped into Montreal Neurological Institute (MNI) space, and the same transformation was used to transfer the coordinates of these peaks into MNI space.

Two-sample *t* tests were used in SPM5 to examine the difference in absolute perfusion between patients (AD and FTLD) and controls using the spatially normalized CBF maps. Global CBF values, disease duration, and age at onset were included in the model as nuisance covariates. Imaging results were thresholded at a false detection rate (FDR) of 0.05.[24] For maps that did not survive FDR correction, we used an uncorrected threshold of $p < 0.005$ with a cluster threshold of 40 voxels, corresponding to 3 times the smoothing kernel.

RESULTS

CBF difference between patients with FTLD and controls. Figure 1A shows the CBF difference between patients with FTLD and controls, and the coordinates of the peaks showing the local maximum CBF differences are summarized in table 2. Significantly reduced absolute CBF in FTLD compared with healthy aging was found in dorsolateral prefrontal cortex (dlPFC) bilaterally and right inferior frontal cortex (iFC), including orbital frontal cortex (OFC) and insula. We also observed areas of increased absolute perfusion in FTLD in medial parietal cortex(PC)/precuneus (PRC) and posterior cingulate cortex (PCC). A similar CBF pattern was seen in the subgroup of 4 patients with autopsy-confirmed FTLD (figure e-1 and table e-1 on the *Neurology*® Web site at www.neurology.org).

CBF difference between patients with AD and controls. Figure 1B shows the differences in absolute CBF between patients with AD and healthy seniors, and the coordinates of the peak locations are summarized in table 2. At a FDR-corrected significance level of $p < 0.05$, hypoperfusion in AD was demonstrated in medial PC/PRC, left lateral PC, and left middle temporal cortex (mTC) and inferior temporal cortex. Significant hyperperfusion was found in right dorsal ACC (dACC), right dlPFC, and right insula. We observed a similar pattern of changed perfusion in patients with autopsy-confirmed AD (figure e-2 and table e-2).

CBF difference between patients with FTLD and patients with AD. Figure 2 shows the results of a direct comparison of perfusion in patients with FTLD and AD, and the coordinates of the peaks are listed in table 3. At an FDR-corrected significance level of $p < 0.05$, lower CBF in FTLD than in AD was found in medial iFC including OFC, left lateral iFC, dACC, and left dlPFC. Significantly lower CBF in AD than in FTLD was found in PCC, medial PC/PRC, left lateral PC, and left mTC and superior temporal cortex.

DISCUSSION

Quantitative perfusion obtained with cASL MRI in patients with autopsy or CSF biomarkers revealed doubly dissociated patterns of hypoperfusion in AD and FTLD. Significantly reduced frontal CBF was seen in FTLD, and significant temporal-parietal hypoperfusion was found in AD. Moreover, we observed distinct areas of significant hyperperfusion in FTLD and AD. These observa-

Figure 1 Statistical parametric map of significant cerebral blood flow differences between patients and controls

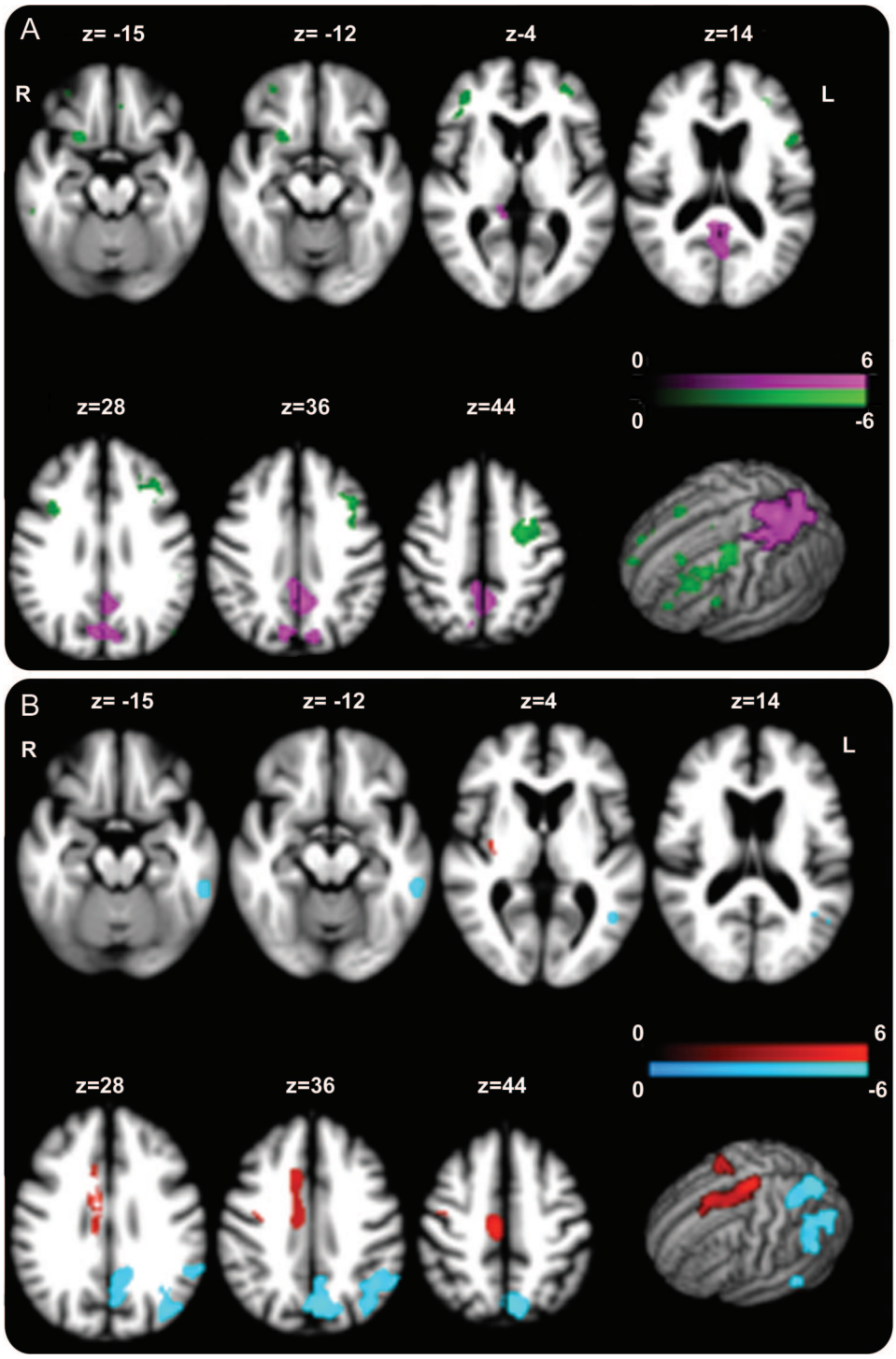

(A) Patients with frontotemporal lobar degeneration (FTLD). The significance level used for thresholding the maps in A was $p < 0.005$ ($t > 2.66$, uncorrected). Green = hypoperfusion and purple = hyperperfusion in FTLD. (B) Patients with Alzheimer disease (AD). The significance level used for thresholding the maps in B was $p < 0.05$ ($t > 3.4$, with false discovery rate correction). Turquoise = hypoperfusion and red = hyperperfusion in AD.

tions underline the potential usefulness of ASL in distinguishing between FTLD and AD.

Direct comparisons of ASL with ^{15}O-PET show that MRI and PET methods for measuring CBF are highly comparable.[25] Moreover, an MRI-based blood flow technique like ASL is more widely available than PET because it can be obtained with standard clinical MRI equipment, ASL is less expensive, and ASL

Table 2 Regional hypoperfusion and hyperperfusion in patients with FTLD and AD relative to healthy seniors

Anatomical locus	Coordinates x	y	z	t Score	Uncorrected peak p value[a]
Frontotemporal lobar degeneration					
Hypoperfusion					
Left dlPFC	−46	28	30	4.27	3.5e-5
Left dlPFC	−41	54	10	3.35	7.0e-4
Right dlPFC	50	10	30	3.18	1.2e-3
Right dlPFC	40	56	8	3.17	1.2e-3
Right iFC	22	19	−19	3.61	3.1e-4
Right iFC	36	60	−8	3.33	7.5e-4
Hyperperfusion					
Medial PC/PRC	−3	−48	45	4.38	2.4e-5
PCC	−8	−58	40	4.25	3.8e-5
Alzheimer disease					
Hypoperfusion					
Medial PC/PRC	−2	−60	38	6.29[b]	1.4e-7
Left lateral PC	−46	−70	34	5.72[b]	8.2e-7
Left mTC/iTC	−60	−44	−20	4.69[b]	1.9e-5
Hyperperfusion					
Right dACC	8	−1	38	5.97[b]	3.9e-7
Right dlPFC	33	−10	42	4.12[b]	1.1e-4
Right insula	36	−12	6	3.93[b]	1.9e-4

Abbreviations: AD = Alzheimer disease; dACC = dorsal anterior cingulate cortex; dlPFC = dorsolateral prefrontal cortex; FTLD = frontotemporal lobar dementia; iFC = inferior frontal cortex; iTC = inferior temporal cortex; mTC = middle temporal cortex; PC = parietal cortex; PCC = posterior cingulate cortex; PRC = precuneus.
[a] All contrasts significant at $p < 0.005$ uncorrected for multiple comparisons.
[b] Contrast survived false detection rate-corrected multiple comparisons at $p < 0.05$.

avoids exposure to ionizing radiation. Importantly, CBF techniques seem to validly reflect neuronal glucose metabolism as measured by FDG-PET because FDG-PET and ^{15}O-PET yield similar results in healthy seniors and in patients with neurodegenerative conditions.[26] Using ASL to measure CBF, we found significantly reduced perfusion in inferior, dorsolateral, medial, and insular regions of the frontal lobe in FTLD. These areas correspond to regions of known disease in FTLD, based on regional autopsy findings.[4] A similar anatomical distribution of hypoperfusion was seen in the subgroup of patients with FTLD with autopsy-confirmed disease. One previous study of FTLD with ASL demonstrated superior frontal hypoperfusion,[10] partially corresponding to our findings. The discrepancies between this study and our findings may have been due in part to partial coverage of the brain and use of a less sensitive pulsed ASL sequence in prior work. The regions of hypoperfusion in both studies correspond to areas of significant atrophy in structural MRI studies of FTLD.[4,5] In the present study, we used 2 approaches to correct for morphometric effects on regional CBF. The PVE correction adjusted for the partial volume of white matter in gray matter voxels[10] and the Jacobian-based spatial-transformation correction adjusted for the compression or expansion of brain regions due to normalization to the local template.[18] The latter step was reported in a study that found more significant hyperperfusion in hippocampus in patients with mild AD after correction.[23] However, similar effects but with a slightly reduced significance level were obtained if the second Jacobian-based correction was not applied. Accordingly, the observed hypoperfusion likely reflects functional changes beyond those that can be attributed to atrophy alone. Furthermore, PVE cannot easily explain the observed regions of hyperperfusion.

Patients with FTLD showed significant hyperperfusion in parietal cortex and precuneus. These areas tend to show significant disease only late in the course of FTLD, whereas the patients participating in this study were relatively early in their disease course. Hyperperfusion may be possible because of preserved connectivity in unaffected intrinsic connectivity networks in FTLD.[27] The significance of observed hyperperfusion remains to be established. One possibility is that there is a dissociation between vascular perfusion measured by ASL and neuronal metabolic consumption of substrate. Partial perfusion-metabolic uncoupling can occur if there is a change in vascular diameter or a mitochondrial disorder of neuronal metabolism, but neither is associated with FTLD. Another possibility is related to the concept of "reserve" or "compensation" in neurodegenerative conditions like FTLD.[28] From this perspective, neuronal integrity in these areas is beginning to be stressed by the incipient accumulation of abnormal neuronal histopathologic inclusions, and up-regulation of regional cortical activity may attempt to compensate in part for these early challenges to regional neuronal functioning. A related account implicates increased activity in response to partial deafferentation as a result of disease in frontal areas that compromises projections to these hyperperfused regions. This would be consistent with imaging observations of diffusion tensor imaging defects in WM projections in FTLD.[29] It is difficult to assess these hypotheses because direct tissue evidence of modest disease burden in hyperperfused areas is difficult to obtain. Indirect evidence can be acquired in future work that assesses the fate of CBF in hyperperfused areas in longitudinal ASL observations.

Areas of significant hypoperfusion in AD involved a different anatomical distribution than areas showing significantly reduced CBF in FTLD. Patients with AD thus showed significant hypoperfusion in posterior brain regions, including parietal,

Figure 2 Statistical parametric map of significant cerebral blood flow differences between patients with FTLD and AD

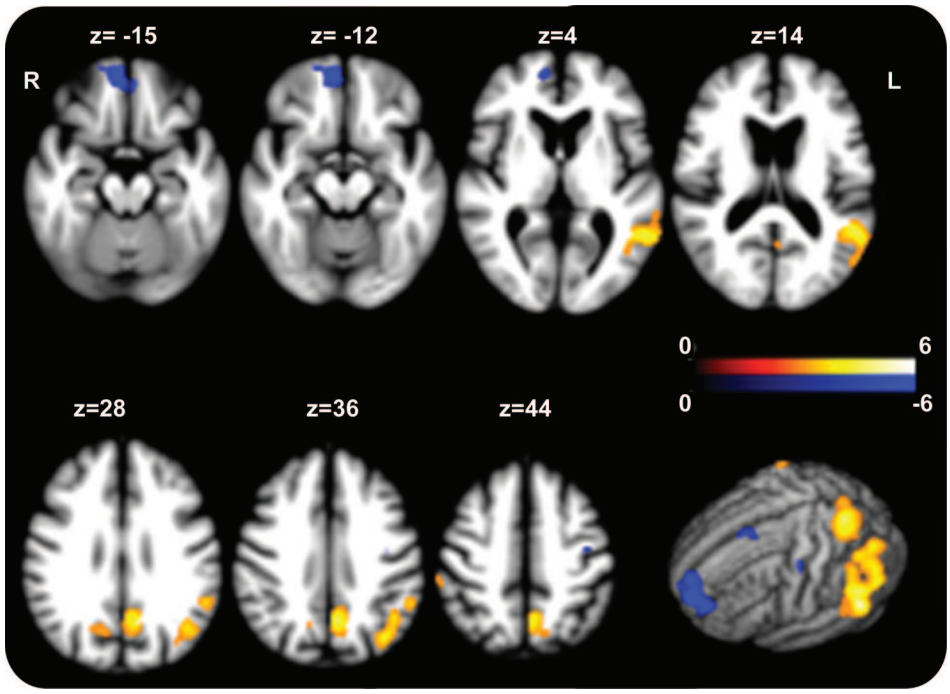

The significance level used for thresholding the statistical parametric map is $p < 0.05$ ($t > 3.2$, with false discovery rate correction). Yellow indicates significantly reduced perfusion in Alzheimer disease (AD) compared with frontotemporal lobar degeneration (FTLD); blue indicates significantly reduced perfusion in FTLD compared with AD.

temporal, and precuneus regions. This corresponds to areas of significant histopathologic burden in autopsy-confirmed AD,[30] and hypoperfusion was observed in these areas in autopsy-confirmed cases of AD. Previous ASL studies of AD have shown a similar anatomical pattern of hypoperfusion.[10,31-34] We did not observe medial temporal hypoperfusion, as reported in some of this work. Cross-sectional studies thus have suggested that patients with very mild AD and mild cognitive impairment (MCI) may have hippocampal hyperperfusion.[32,33] This would be consistent with other work showing increased medial temporal activation during performance of memory-related tasks in MCI[35] and hippocampal neuronal hypertrophy in asymptomatic AD.[36] One longitudinal study related hippocampal activation to subsequent cognitive decline in AD.[37] There may have been some averaging across cases with hypoperfusion and hyperperfusion of the medial temporal region in our series. Moreover, because some patients classified as AD in our series had clinical features more consistent with bvFTD or PPA, there may have been little change in medial temporal perfusion early in the course of disease. Additional work is needed in larger groups of patients to establish more precisely the fate of medial temporal perfusion in mild AD.

We also observed areas of significant cortical hyperperfusion in AD. This included areas of the frontal lobe and lateral temporal lobe, regions where disease emerges later in the course of AD than the medial temporal lobe.[30] Cortical hyperperfusion has been described in several previous studies.[32,33] This may be related in part to a similar mechanism implicated in the neuronal hypertrophy observed in the anterior cingulate of asymptomatic AD.[36] We also cannot rule out the contribution of partial deafferentation due to degraded WM projections from diseased areas.[38,39]

We observed a double dissociation between AD and FTLD, emphasizing the potential usefulness of ASL as a diagnostic modality. PET studies have repeatedly demonstrated frontal hypometabolism in bvFTD and parietal hypometabolism in AD, as we observed, although comparative studies such as ours are rare. Moreover, one recent PET study described parietal-occipital hypermetabolism in bvFTD and frontotemporal hypermetabolism in AD when adjusting for global glucose metabolism,[40] consistent with our findings using ASL.

Several limitations in our study should be kept in mind. Regional perfusion patterns may depend in part on disease duration, and the slightly longer disease duration in FTLD may have confounded our analysis. CSF AD biomarkers were used as surrogate markers of pathology rather than true neuropathologic analysis for many patients. Despite the high

Table 3 Regional perfusion differences in direct contrasts of patients with AD and FTLD

Anatomical locus	Coordinates x	y	z	t Score[a]
AD < FTLD				
PCC	−2	−47	29	3.4
Medial PC/PRC	−2	−67	38	5.05
Left lateral PC	−49	−68	29	4.64
Left mTC	−63	−45	3	5.55
Left sTC	−58	−45	17	5.12
FTLD < AD				
Medial iFC	6	51	−13	5.59
Left iFC	−41	51	−7	3.43
dACC	12	9	34	3.65
Left dlPFC	−36	−12	41	3.74

Abbreviations: AD = Alzheimer disease; dACC = dorsal anterior cingulate cortex; dlPFC = dorsolateral prefrontal cortex; FTLD = frontotemporal lobar dementia; iFC = inferior frontal cortex; mTC = middle temporal cortex; PC = parietal cortex; PCC = posterior cingulate cortex; PRC = precuneus cortex; sTC = superior temporal cortex.
[a] All contrasts survived false detection rate–corrected multiple comparisons at $p < 0.05$.

sensitivity and specificity of CSF AD biomarkers, there is currently no biomarker that positively identifies FTLD pathology, and patients may have been misclassified by CSF biomarkers alone. A definitive study is needed in the future to determine the usefulness of ASL as a biomarker using pathologically confirmed cases of AD and FTLD. With these caveats in mind, the double dissociation between AD and FTLD that we observed is consistent with the hypothesis that simultaneous analysis of susceptible and resistant brain regions can improve the differential diagnosis of underlying pathology in AD and FTLD clinical syndromes.

DISCLOSURE

Dr. Hu has a patent pending re: Cerebrospinal Fluid and Plasma Biomarkers for AD; and receives research support from the American Academy of Neurology Foundation (Clinical Research Training Fellowship). Dr. Wang reports no disclosures. Dr. Lee has received funding for travel or speaker honoraria from Takeda Pharmaceutical Company Limited, Genentech, Inc. and Pfizer Inc; serves on the editorial boards of *Laboratory Investigation*, *Neurorehabilitation and Neural Repair*, *NeuroSignals*, *Neuron*, and *Experimental Neurology* and on the Board of Reviewing Editors for *Science Magazine*; holds and has patents pending re: Modified Avidin-Biotin Technique, Method of Stabilizing Microtubules to Treat Alzheimer's Disease, Method of Screening for Alzheimer's Disease or Disease Associated With the Accumulation of Paired Helical Filaments, Compositions and Methods for Producing and Using Homogeneous Neuronal Cell Transplants, Animal Model for Alzheimer's Disease, Method of Identifying, Diagnosing and Treating α-Synuclein Positive Neurodegenerative Disorders, Identification and Characterization of AB-Negative Plaques and Methods of Diagnosing Alzheimer's Disease, and Mutation-Specific Functional Impairments in Distinct Tau Isoforms of Hereditary Frontotemporal Dementia and Parkinsonism Linked to Chromosome-17; and receives research support from the NIH (NIA P30-AG 009215-19 [Project Leader]) and Ware Benaroya. Dr. Trojanowski has received funding for travel and honoraria from Takeda Pharmaceutical Company Ltd.; serves as an Associate Editor of *Alzheimer's & Dementia*; may accrue revenue on patents re: Modified Avidin-Biotin Technique, Method of Stabilizing Microtubules to Treat Alzheimer's Disease, Method of Detecting Abnormally Phosphorylated Tau, Method of Screening for Alzheimer's Disease or Disease Associated With the Accumulation of Paired Helical Filaments, Compositions and Methods for Producing and Using Homogeneous Neuronal Cell Transplants, Rat Comprising Straight Filaments in Its Brain, Compositions and Methods for Producing and Using Homogeneous Neuronal Cell Transplants to Treat Neurodegenerative Disorders and Brain and Spinal Cord Injuries, Diagnostic Methods for Alzheimer's Disease by Detection of Multiple MRNAs, Methods and Compositions for Determining Lipid Peroxidation Levels in Oxidant Stress Syndromes and Diseases, Compositions and Methods for Producing and Using Homogenous Neuronal Cell Transplants, Method of Identifying, Diagnosing and Treating α-Synuclein Positive Neurodegenerative Disorders, Mutation-Specific Functional Impairments in Distinct Tau Isoforms of Hereditary Frontotemporal Dementia and Parkinsonism Linked to Chromosome-17: Genotype Predicts Phenotype, Microtubule Stabilizing Therapies for Neurodegenerative Disorders, and Treatment of Alzheimer's and Related Diseases With an Antibody; and receives research support from the NIH (NIA P01 AG 09215-20 [PI], NIA P30 AG 10124-18 [PI], NIA PO1 AG 17586-10 [Project 4 Leader], NIA 1PO1 AG-19724-07 [Core C Leader], NIA 1 U01 AG 024904-05 [Co-PI Biomarker Core Laboratory], NINDS P50 NS053488-02 [PI], NIA UO1 AG029213-01 [Coinvestigator], RC2NS069368 [PI], RC1AG035427 [PI], and NIA P30AG036468 [PI]) and the Marian S. Ware Alzheimer Program. Dr. Detre serves on a scientific advisory board of Pittsburgh NMR Center; serves as an Associate Editor of the *Journal of Neuroimaging*; serves as a consultant for Pfizer Inc; receives research support from Wyeth, AstraZeneca, Pfizer Inc, the National Science Foundation, and the NIH (R01 MH080729 [PI], K24 NS058386 [PI], P30 NS045839 [PI], T32 NS054575 [PI], R01 NS060653 [Coinvestigator], R01 NS061572 [Coinvestigator], P41 RR002305 [PI], R24 HD050836 [PI], R24 HD050838 [Coinvestigator], R01 NS057400 [Coinvestigator], R01 DK085615 [Coinvestigator], R01AG034682 [Coinvestigator], R21 DA025882 [Coinvestigator], R01 HL102119 [Coinvestigator], R03 DA027098 [Coinvestigator], and R24 HD050836 [Coinvestigator]); is an inventor on a patent re: ASC Perfusion MRI and receives royalties from the University of Pennsylvania for its licensure; and has acted as a witness or consultant in legal proceedings. Dr. Grossman serves on a scientific advisory board for Allon Therapeutics Inc.; serves as Editor of *Cognitive and Behavioral Neurology*; serves as a consultant for Pfizer Inc, Forest Laboratories, Inc., and Allon Therapeutics Inc.; and receives research support from the NIH (AG17586 [Project and Core Leader], AG15116 [PI], NS44266 [PI], and NS53488 [Project Leader]).

Received March 17, 2010. Accepted in final form May 14, 2010.

REFERENCES

1. Alladi S, Xuereb J, Bak T, et al. Focal cortical presentations of Alzheimer's disease. Brain 2007;130:2636–2645.
2. Grossman M. Primary progressive aphasia: clinicopathological correlations. Nat Rev Neurol 2010;6:88–97.
3. Graham A, Davies R, Xuereb J, et al. Pathologically proven frontotemporal dementia presenting with severe amnesia. Brain 2005;128:597–605.
4. Grossman M, Libon DJ, Forman MS, et al. Distinct antemortem profiles in patients with pathologically defined frontotemporal dementia. Arch Neurol 2007;64:1601–1609.
5. Whitwell JL, Jack CR Jr, Pankratz VS, et al. Rates of brain atrophy over time in autopsy-proven frontotemporal dementia and Alzheimer disease. Neuroimage 2008;39:1034–1040.

6. Whitwell JL, Jack CR Jr, Parisi JE, et al. Rates of cerebral atrophy differ in different degenerative pathologies. Brain 2007;130:1148–1158.
7. Nordberg A, Rinne JO, Kadir A, Langstrom B. The use of PET in Alzheimer disease. Nat Rev Neurol 2010;6:78–87.
8. Raichle ME. Behind the scenes of functional brain imaging: a historical and physiological perspective. Proc Natl Acad Sci USA 1998;95:765–772.
9. Alsop DC, Detre JA. Multisection cerebral blood flow MR imaging with continuous arterial spin labeling. Radiology 1998;208:410–416.
10. Du AT, Jahng G-H, Hayasaka S, et al. Hypoperfusion in frontotemporal dementia and Alzheimer disease by arterial spin labeling MRI. Neurology 2006;67:1215–1220.
11. McKhann G, Drachman D, Folstein M, Katzman R, Price D, Stadian EM. Clinical diagnosis of Alzheimer's disease: report on the NINCDS-ADRDA work group under the auspices of the Department of Health and Human Services Task Force on Alzheimer's disease. Neurology 1984;34:939–944.
12. McKhann G, Trojanowski JQ, Grossman M, Miller BL, Dickson D, Albert M. Clinical and pathological diagnosis of frontotemporal dementia: report of a work group on frontotemporal dementia and Pick's disease. Arch Neurol 2001;58:1803–1809.
13. Bian H, van Sweiten JC, Leight S, et al. Cerebrospinal fluid biomarkers in frontotemporal lobar degeneration with known pathology. Neurology 2008;70:1827–1835.
14. Wang JJ, Zhang Y, Wolf RL, Roc AC, Alsop DC, Detre JA. Amplitude modulated continuous arterial spin labeling perfusion MR with single coil at 3T: feasibility study. Radiology 2005;235:218–228.
15. Wang Z, Aguirre GK, Rao H, et al. Empirical optimization of ASL data analysis using an ASL data processing toolbox: ASLtbx. Magn Reson Imaging 2008;26:261–269.
16. Press WH, Teukolsky SA, Vetterling WT, Flannery BP. Numerical Recipes: The Art of Scientific Computing. 3rd ed. New York: Cambridge University Press; 2007.
17. Wang Z, Childress AR, Wang J, Detre JA. Support vector machine learning-based fMRI data group analysis. Neuroimage 2007;36:1139–1151.
18. Ashburner J. A fast diffeomorphic image registration algorithm. Neuroimage 2007;38:95–113.
19. Leenders KL, Perani D, Lammertsma AA, et al. Cerebral blood flow, blood volume and oxygen utilization: normal values and effect of age. Brain 1990;113(pt 1):27–47.
20. Haacke EM, Brown RW, Thompson MR, Venkatesan R. Magnetic Resonance Imaging: Physical Principles and Sequence Design. New York: John Wiley and Sons; 1999.
21. Buxton RB. Introduction to Functional Magnetic Resonance Imaging. New York: Cambridge University Press; 2002.
22. Stanisz GJ, Odrobina EE, Pun J, et al. T1, T2 relaxation and magnetization transfer in tissue at 3T. Magn Reson Med 2005;54:507–512.
23. Alsop DC, Casement M, de Bazelaire C, Fong T, Press DZ. Hippocampal hyperperfusion in Alzheimer's disease. Neuroimage 2008;42:1267–1274.
24. Genovese CR, Lazar N, Nichols TE. Thresholding of statistical maps in functional neuroimaging using the false discovery rate. Neuroimage 2002;15:870–878.
25. Xu G, Rowley HA, Wu G, et al. Reliability and precision of pseudo-continuous arterial spin labeling perfusion MRI on 3.0†T and comparison with15O-water PET in elderly subjects at risk for Alzheimer's disease. NMR Biomed 2010;23:286–293.
26. Baron JC, Lebrun-Grandie P, Collard P, Crouzel C, Mestelan GT, Bousser MG. Noninvasive measurement of blood flow, oxygen consumption, and glucose utilization in the same brain regions in man by positron emission tomography. J Nucl Med 1982;23:391–399.
27. Seeley WW, Crawford RK, Zhou J, Miller BL, Greicius MD. Neurodegenerative diseases target large-scale human brain networks. Neuron 2009;62:42–52.
28. Stern Y. What is cognitive reserve? Theory and research application of the reserve concept. J Intl Neuropsychological Soc 2002;8:448–460.
29. Borroni B, Brambati SM, Agosti C, et al. Evidence of white matter changes on diffusion tensor imaging in frontotemporal dementia. Arch Neurol 2007;64:246–251.
30. Braak H, Braak E. Neuropathological staging of Alzheimer-related changes. Acta Neuropathol 1991;82:239–259.
31. Alsop DC, Detre J, Grossman M. Assessment of cerebral blood flow in Alzheimer's disease by arterial spin labelling fMRI. Ann Neurol 2000;47:93–100.
32. Alsop DC, Casement M, de Bazelaire C, Fong T, Press DZ. Hippocampal hyperperfusion in Alzheimer's disease. Neuroimage 2008;42:1267–1274.
33. Dai W, Lopez OL, Carmichael OT, Becker JT, Kuller LH, Gach HM. Mild cognitive impairment and Alzheimer disease: patterns of altered cerebral blood flow at MR imaging. Radiology 2009;250:856–866.
34. Johnson NA, Jahng G-H, Weiner MW, et al. Pattern of cerebral hypoperfusion in Alzheimer disease and mild cognitive impairment measured with arterial spin-labeling MR imaging: initial experience. Radiology 2005;234:851–859.
35. Dickerson BC, Salat DH, Greve DN, et al. Increased hippocampal activation in mild cognitive impairment compared to normal aging and AD. Neurology 2005;65:404–411.
36. Iacono D, O'Brien R, Resnick S, et al. Neuronal hypertrophy in asymptomatic Alzheimer disease. J Neuropathol Exp Neurol 2008;67:578–589.
37. Miller SL, Fenstermacher E, Bates J, Blacker D, Sperling R, Dickerson BC. Hippocampal activation in adults with mild cognitive impairment predicts subsequent cognitive decline. J Neurol Neurosurg Psychiatry 2008;79:630–635.
38. Ringman JM, O'Neill J, Geschwind D, et al. Diffusion tensor imaging in preclinical and presymptomatic carriers of familial Alzheimer's disease mutations. Brain 2007;130:1767–1776.
39. Zhang Y, Schuff N, Jahng GH, et al. Diffusion tensor imaging of cingulum fibers in mild cognitive impairment and Alzheimer disease. Neurology 2007;68:13–19.
40. Dukart J, Mueller K, Horstmann A, et al. Differential effects of global and cerebellar normalization on detection and differentiation of dementia in FDG-PET studies. Neuroimage 2010;49:1490–1495.